CHAPTER 5

Thermal Characteristics of Air Flow Over Flat Tube with Ellipsoidal Dimple Surface

5.1 Introduction

In this work, the heat transfer performance of air flow across flat-dimple tube without fins is studied. Both appropriate dimple shape and dimple arrangement which is investigated in Chapter 3 and Chapter 4 are applied on the tube surface. The flat-dimple tube in cross flow was studied in comparison with flat-bare tube. In addition, the effect of tube space of single-row tube bank was also investigated. The heat transfer coefficient of flat-dimpled tube is obtained and reported.

5.2 Experimental setup and procedure

Figure 5.1 presents the schematic sketch of the experimental setup. In this experiment, the air stream generated by a centrifugal air blower was flowed over the heated plate with dimples. The velocity of air stream was controlled by the frequency inverter with the controllable range of 1-4 m/s. The velocity of air stream was measured by a hot wire anemometer with ±0.2 m/s accuracy. The inlet temperature of air stream was measured by 4 sets of T-type thermocouple. The outlet temperature was measured by a T-type thermocouple mesh which consists of 16 thermocouples. Note that all of thermocouples have ±0.1 ^{o}C accuracy. The surface temperature of flat tube was measured by infrared imaging camera with ±2 ^{o}C accuracy. This temperature measuring instrument was also calibrated surface temperature with T-type thermocouple.

The tested section comprises three flat-dimpled tubes which made from steel. The 1,500 watt of plate electric heater was plugged in the tube. The Iron powder was filled between the tube surface and plate heater to avoid air gap. Figure 5.2 present the geometric details of the tested tube, including dimpled geometry. The S_T as shown in the figure is varied from 75 mm, 100 mm, and 125 mm.

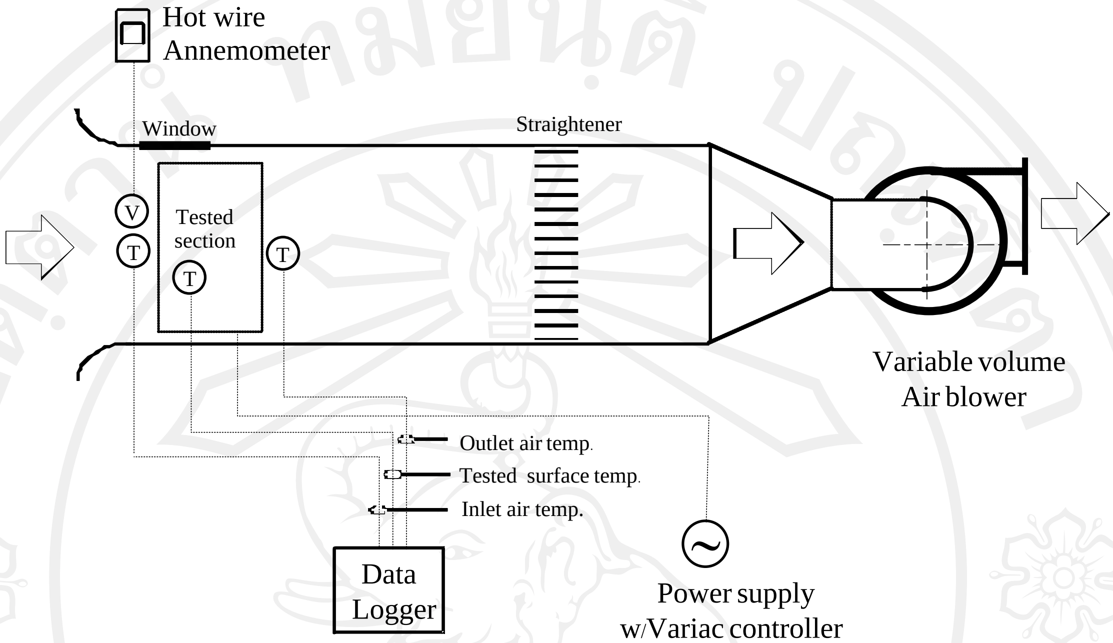

Figure 5.1 Schematic diagram of the experimental setup.

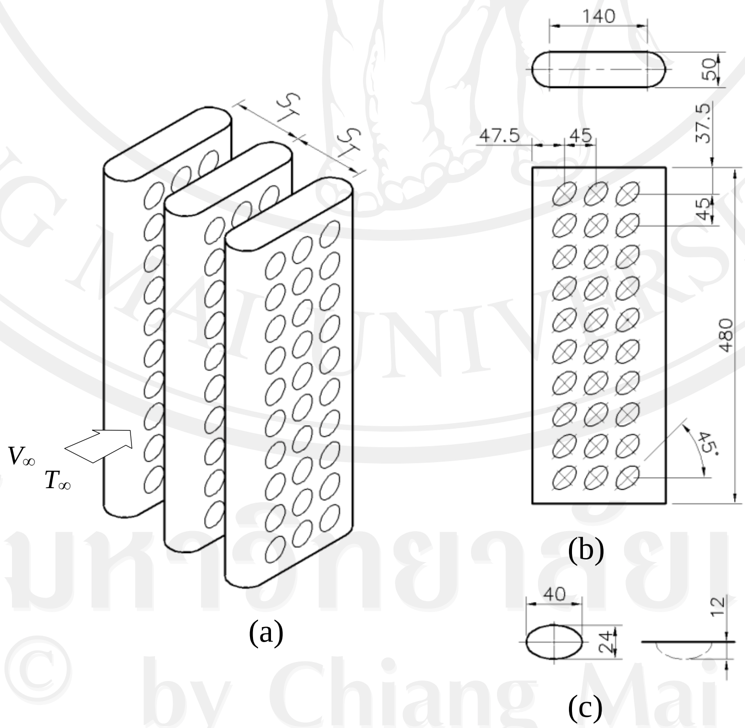

Figure 5.2 Details of: (a) dimpled-flat tube arrangement, (b) individual dimpled-flat tube geometry and (c) individual dimple geometry. All dimensions are in mm.

5.3 Data reduction

5.3.1 Single tube in cross flow

During the experiment, inlet air stream velocity, temperature, tube surface temperature and power supply were measured. The local heat transfer coefficient (h_x) is calculated from

$$h_x = q_s''/(T_s - T_\infty) \tag{5.1}$$

where q'' is surface heat flux. The heat flux is calculated from heat rate level at the tube d flat projected tube surface area, T_s is the local surface temperature and T_∞ is the temperature of inlet air stream flowing over the tested tube respectively.

The average air side heat transfer coefficient (h) of tested tube is determined by integrating all of the area of tube surface as

$$h = q_s''/(T_{s,avg} - T_\infty) \tag{5.2}$$

where $T_{s,avg}$ is the average surface temperature.

The spanwise average Nusselt number (Nu_x) is defined as

$$Nu_x = \frac{hD_h}{k_f} \tag{5.3}$$

where D_h = P/π and P is perimeter of tested tube. k_f is the thermal conductivity of air stream.

Reynolds number ($\mathrm{Re}_{\mathrm{Dh}}$) for air flow is defined as

$$\mathrm{R}e_{\mathrm{Dh}} = \frac{\rho_f V_f D_h}{\mu_f} \tag{5.4}$$

where ρ_f, V_f and μ_f are the density of air, the air frontal velocity and the dynamic viscosity of air stream respectively.

5.3.2 Tube bank in cross flow

During the experiment, inlet and outlet air stream velocity, temperature, the tube surface temperature and power supply were measured. The air side heat transfer rates can be calculated as

$$Q_a = \dot{m}Cp_a(T_{ao} - T_{ai}) \tag{5.5}$$

where Q_a is the heat transfer rate of air flow. For this studied, the average heat transfer rate is the mathematical average of heat transfer rate of the air side and the power supply of heater as

$$Q_{avg} = 0.5(Q_a + Q_e) \tag{5.6}$$

where Q_e is the electrical power supply.

The average air side heat transfer coefficient (*h*) of tested tube is determined by

$$h = Q_{avg} / (NA_s \Delta T_{lm}) \tag{5.7}$$

where ΔT_{lm} is a log-mean temperature difference which is defined as

$$\Delta T_{lm} = \frac{(T_{s,avg} - T_i) - (T_{s,avg} - T_o)}{\ln\left(\dfrac{T_{s,avg} - T_i}{T_{s,avg} - T_o}\right)} \tag{5.8}$$

where *N* is the total number of tubes in the bank, A_s is the surface area of one tube (flat projected surface area only), $T_{s,avg}$ is the average surface temperature, T_i and T_o air the inlet and outlet of air stream respectively.

The average Nusselt number (Nu_D) is defined as

$$Nu_D = \frac{hD}{k_f} \tag{5.9}$$

where *D* is tube width.

Reynolds number ($Re_{D,max}$) for air flow across tube bank is defined as

$$Re_{D,max} = \frac{\rho_f V_{max} D}{\mu_f} \tag{5.10}$$

where V_{max} is a maximum air velocity occurring within the tube bank.

5.4 Results and discussion

5.4.1 Single tube in cross flow

In this part, heat transfer of air flow across the flat tube and flat-dimple tube are studied. Figure 5.3 shows the variation of the local Nusselt number with surface length of cylinder, flat tube and flat-dimple tube in cross flow of air. Starting at the stagnation point, Nu_x of all tube configurations decreases with increasing surface distance as a result of laminar boundary layer development. For cylinder, a minimum is reached at angular dimension is about 80^o and Nu_x increases with angular dimension due to vortex formation in the wake. On the other hand, Nu_x of flat tube and flat-dimple tube reach the minimum at surface distance is about 80 mm, which is on the plain surface. Both flat tube and flat-dimple tube have the same Nu_x trend line with the flat tube lagging by about 9%.

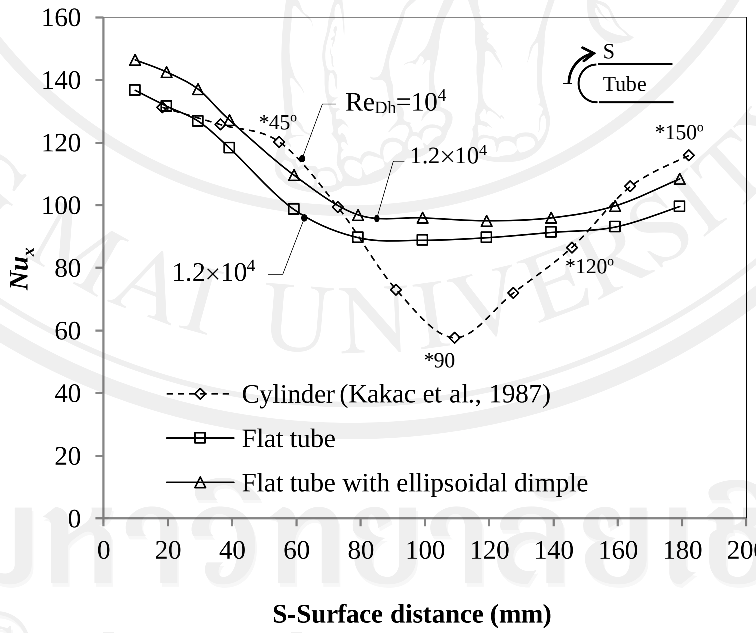

Figure 5.3 Average span-wise Nusselt Number of cylinder, flat tube and flat-dimple tube. (*angular coordinate for cylinder)

Figure 5.4 shows the average air side heat transfer performance of cylinder, flat tube and flat-dimple tube. As shown in the figure, flat tube and flat-dimple tube give the higher heat transfer coefficient than cylinder in same D_h and at all frontal velocities. Over a range of frontal velocity, enhancement of the average heat transfer coefficient is about 1.5 and 1.63 times for flat tube and flat-dimple tube respectively, compare to cylinder.

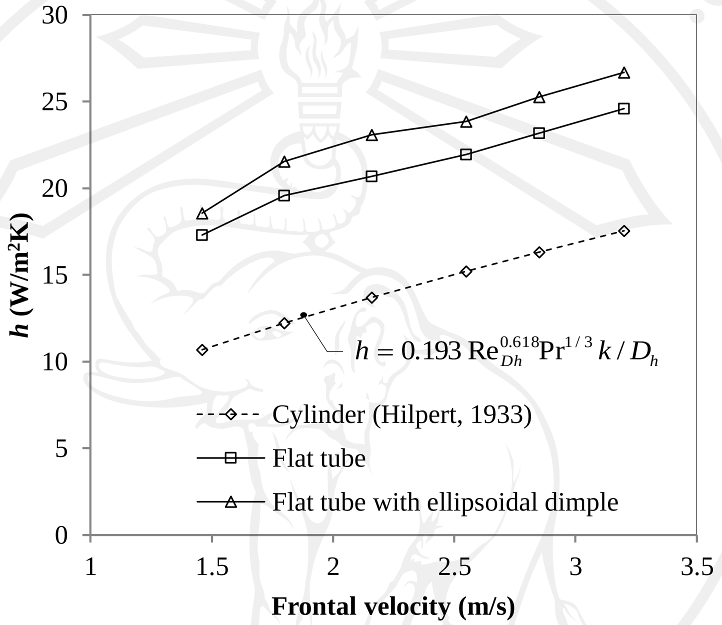

Figure 5.4 Average heat transfer coefficient for cylinder, flat tube and flat-dimple tube.

5.4.2 Tube bank in cross flow

In this part, heat transfer of air flow across single row tube bank is investigated. Tube bank comprises of three flat-dimple tube. The tube pitch (S_T/D) is varied from 1.5, 2 and 2.5. Figure 5.5 shows the effect of S_T/D to the air side heat transfer performance. As seen in the Figure, Average heat transfer coefficient decrease as S_T/D increase due to the maximum air velocity passing the tube bank is increased with decreasing of tube pitch.

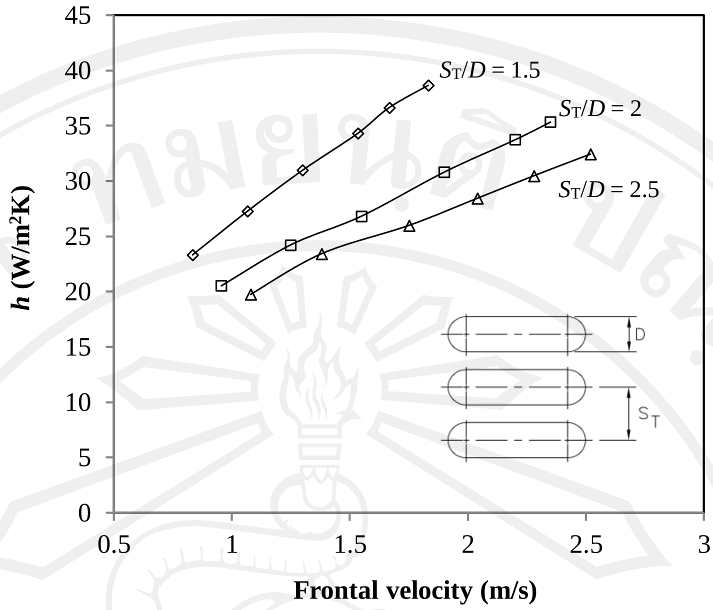

Figure 5.5 Average heat transfer coefficient to frontal velocity for tube bank.

5.4.3 Empirical correlation

From the previous results, the multiple linear regression technique is performed to obtain the relevant correlation. The corresponding correlation is given as follows;

$$Nu_D = 0.1983\,\mathrm{Re}_{D,\max}^{0.618}\,\mathrm{Pr}^{1/3} \tag{5.11}$$

Figure 5.6 shows the comparison of *Nu* of the experimental results with the proposed correlation. For the Nusselt number correlation Eq. (11) can predicts 95.1% and of the experimental data with ±5%. The standard deviation of the correlation Eq. (11) is 1.8%.

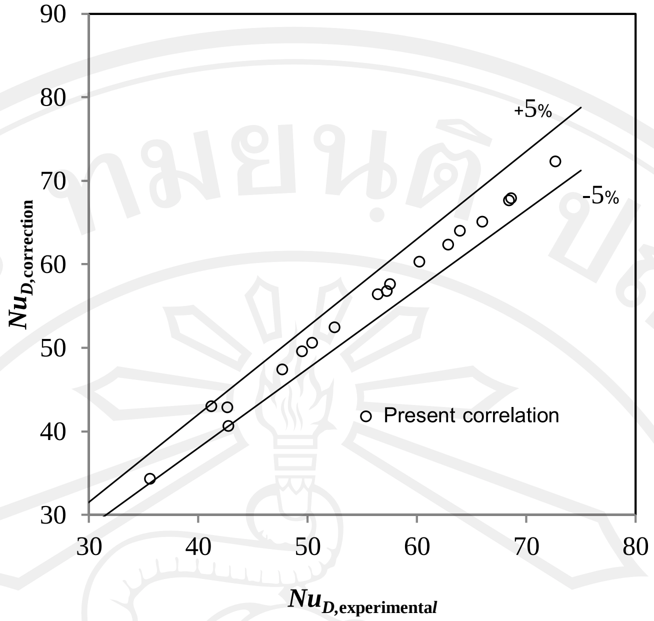

Figure 5.6 Comparison of *Nu* correlations with experimental data.

5.5 Summary and conclusion

The present study reports the heat transfer performance of air flow over the flat tube, flat-dimple tube and flat-dimple tube bank. The effect of tube pitch is examined. On the basis of previous discussions, the conclusions are made:

1) Air side heat transfer performance of flat tube and flat-dimple tube is augmented at all frontal velocity. The heat augmentation is approximately 60%.

2) Heat transfer enhancement is about 1.5 and 1.63 times for flat tube and flat-dimple tube respectively, compare to cylinder in the same surface area condition.

3) Correlation of the present experiment is developed. The proposed correlation yields fairly good predictive ability against the present test data.